Bull Earthquake Eng (2014) 12:1977–1997
DOI 10.1007/s10518-013-9499-3

ORIGINAL RESEARCH PAPER

Performance of buildings with masonry infill walls during the 2011 Lorca earthquake

Lutz Hermanns · Alberto Fraile · Enrique Alarcón · Ramón Álvarez

Received: 24 February 2012 / Accepted: 29 July 2013 / Published online: 9 August 2013

Abstract On Wednesday 11th May 2011 at 6:47 pm (local time) a magnitude 5.1 Mw earthquake occurred 6 km northeast of Lorca with a depth of around 5 km. As a consequence of the shallow depth and the small epicentral distance, important damage was produced in several masonry constructions and even led to the collapse of one of them. Pieces of the facades of several buildings fell down onto the sidewalk, being one of the reasons for the killing of a total of 9 people. The objective of this paper is to describe and analyze the failure patterns observed in reinforced concrete frame buildings with masonry infill walls ranging from 3 to 8 floors in height. Structural as well as non-structural masonry walls suffered important damage that led to redistributions of forces causing in some cases the failure of columns. The importance of the interaction between the structural frames and the infill panels is analyzed by means of non-linear Finite Element Models. The resulting load levels are compared with the member capacities and the changes of the mechanical properties during the seismic event are described and discussed. In the light of the results obtained the observed failure patterns are explained. Some comments are stated concerning the adequacy of the numerical models that are usually used during the design phase for the seismic analysis.

Keywords Lorca earthquake · Masonry · Non-linear Finite Element simulation · Infill · Interaction · Column shear demand

1 Introduction

The city of Lorca is located in the south-east of Spain, an area of low to medium seismic hazard. According to the current Spanish Seismic Design Code (Norma de Construcción Sismoresistente 2002) the spectral acceleration at zero period considering a return period of 500 years results in 12 % g (for a stiff soil site). There is a station of the National Seismic

L. Hermanns (✉)· A. Fraile · E. Alarcón · R. Álvarez
Department of Structural Mechanics and Industrial Constructions, School of Industrial Engineering (ETSII), Technical University of Madrid (UPM), C/ Jose Gutierrez Abascal, 2, 28006 Madrid, Spain
e-mail: lhermanns@etsii.upm.es

Table 1 Peak Ground Accelerations registered at Lorca Station (Instituto Geográfico Nacional 2011)

Direction	PGA (cm/s^2)
East–West	150.3
North–South	357.9
Vertical	114.9

Fig. 1 Street covered with rubble of damaged buildings

Network located at only 3 km from the epicenter that registered the peak accelerations presented in Table 1.

The earthquake damaged many buildings in the town of Lorca however, in terms of catastrophic failures the situation did not reach dramatic proportions. Actually only one building collapsed; a recently built apartment house. The situation on the streets was quite similar throughout the whole town.

As can be seen in Fig. 1 rubble was strewn across the streets from damaged buildings. Actually pieces of the facades that fell down during the earthquake injured a lot of persons. In some occasions façade infill panels located at upper floors and roof parapets collapsed and fell onto the ground. Two different failure mechanisms are thought to be responsible for their collapse.

In the case of roof parapets, chimneys and to a minor extent infill panels at upper floors the failure was caused by inertia forces acting out-of-plane. Throughout this paper the terms infill wall and masonry infill wall are used synonymously to refer to the non-structural masonry infill panel of a reinforced concrete frame. It is well known that the resistance of masonry infill walls to out-of-plane moments is much lower than that of structural frames. As a consequence the interaction between the frames and the infill panels is very limited in this particular loading scenario as the failure of the infill panel changes the structural properties at a very low load level. Regarding unreinforced roof parapet walls some codes (FEMA E-74 2011) point out the significant falling hazard related to this type of architectural components. Figure 2 shows one of the parapets that partially collapsed confirming thereby the importance of studying the seismic behavior of non-structural components.

Fig. 2 Building with a partially collapsed parapet wall

The structure of this particular building did not suffer significant damage whereas the roof parapet almost completely collapsed. This type of incoherence in terms of the seismic behavior of different components of the same building is unacceptable.

On lower floors the failure of masonry infill panels was caused by excessive in plane loads, displacements of the frame structure (see Fig. 3) and in some cases by pounding of adjacent buildings.

In these cases both the stiffness of the framing structure and that of the masonry infill are comparable and the resistance of the infill panels is significant permitting thereby important interactions like a force transfer from the slightly cracked masonry infill wall to the surrounding frame structure.

Although in some cases a combination of the two different failure mechanisms described above was observed, in general, the first one was more often observed on upper floors and the second one on lower floors.

2 Seismic behavior of unreinforced roof parapet walls

As already mentioned in the introduction the forces that act on roof parapets are the result of their mass in combination with the acceleration at roof level. It is important to note that the acceleration at roof level may be significantly higher than that at ground level due to the dynamic properties of the building. In Fig. 4 two acceleration time histories are shown.

The blue curve corresponds to the North–South component registered at the Lorca station of the National Seismic Network and the red one corresponds to the estimated acceleration at roof level of a typical eight-floor building with fundamental period of 0.72 s. The maximum acceleration at roof level almost reaches 1 g. Considering only the first vibration mode of the parapet wall the maximum out-of-plane moment builds up at the contact between roof and parapet wall. Unfortunately the bending moment capacity at this contact surface is usually smaller than the resulting demand and the consequences can be seen in Fig. 2. The amplification effect of the building may also be observed in Fig. 5 where the corresponding response spectra of the acceleration time histories at ground (blue curve) and at roof level (red curve) are displayed.

Fig. 3 Damaged masonry infill walls at ground floor

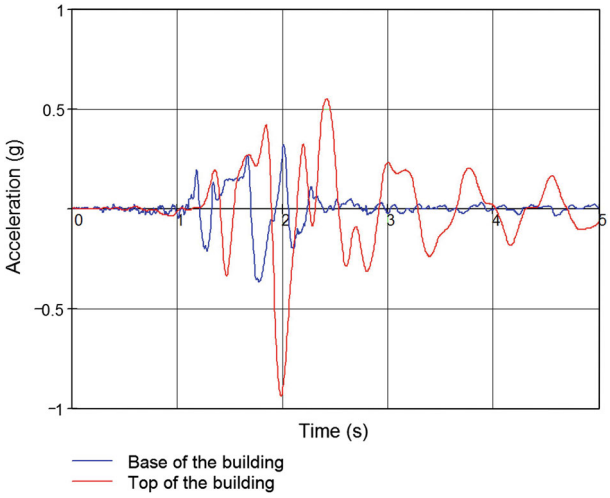

Fig. 4 Acceleration time histories at ground level (*blue curve*) and at roof level (*red curve*)

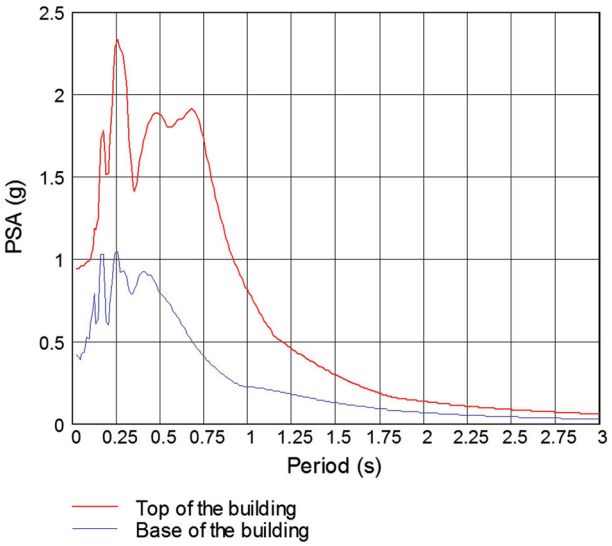

Fig. 5 Response spectrum at ground level (*blue curve*) and floor response spectrum at roof level (*red curve*)

Fig. 6 Collapsed chimney on a flat roof

At this point it should be remembered that these response spectra correspond to one horizontal component of a magnitude Mw 5.1 earthquake and its effects at roof level of a typical eight-floor building!

Not only parapet walls failed at this load level but also chimneys as can be seen in Fig. 6.

3 Failure patterns of masonry infill walls

After the earthquake a damage assessment was performed revealing that most of the damage may be classified as well known failure modes due to the interaction between the frame

Fig. 7 **a** Buildings with a soft-storey, **b** severely damaged column

structure and interior partitions or façade elements. A distinction of these failure modes may be drawn depending on whether the initial combination of the lateral resistive elements is responsible or whether the progressive failure of some of them and the accompanying change of the stiffness distribution leads to an excessive seismic demand. The following 5 points belonging to the first group have been observed in Lorca.

- Some buildings didn't seem to have effective mechanisms to resist lateral loads. However, most of them did not suffer excessive damage. In these cases the stiffness of the masonry infill panels add to the one of the frame structure and the infill panels resisted quite well. The damage distribution was similar to the one observed in buildings with an effective lateral load resistance mechanism.
- Asymmetrical horizontal stiffness distribution leading to torsion moments. This was quite often the case in corner buildings of apartment blocks. The only building that collapsed during the earthquake falls into this category. Other corner buildings with asymmetrical horizontal stiffness distribution suffered substantial damage.
- Soft storey mechanisms due to infill panels with lower stiffness at the ground floor level and panels with higher stiffness at upper floors (see Fig. 7a).
- Masonry infilling effect on frame columns (see Fig. 7b). The horizontal displacements of the frame columns are restricted due to the presence of the infill wall. The reduced height of the column increases the forces the column experiences during a seismic event.
- Shear force concentration in combined systems consisting of RC columns and masonry infill walls (see Fig. 8). In order to estimate realistic shear forces during the design phase it is crucial to take the stiffness of the masonry infill wall into account however, quite often infills are not considered in the structural building model that is used for the seismic response analysis. It is quite common that only one infilled bay exists at ground level. In this case the infill is usually part of the elevator core walls.

In the context of this paper, the term beam-column junction is used to refer to the section of the column just below the soffit of the beam.

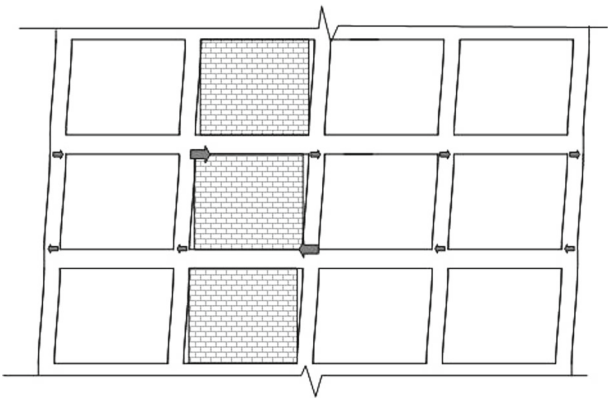

Fig. 8 Shear force concentrations at beam–column junctions due to the presence of masonry infill

Regarding the second group the following 2 points have been observed in Lorca.

- Formation of soft storey mechanisms due to the progressive degradation of the infill panels located at ground floor levels.
- Column failure due to interaction forces between the infill walls and the RC columns. The adjacent frame columns are usually not designed considering different failure modes of the masonry infill walls and the resulting force redistribution.

In the following the last two points are further developed.

3.1 Formation of soft-storey mechanisms

In order to study the formation of a soft-storey mechanism the example of a typical eight-floor apartment building is used. In one direction there are four 5 m span bays and in the other the spacing between adjacent columns is 6 m. The height of the ground floor is 4.25 m and that of the others 3.25 m. The storey masses were estimated using approximate formulas and the columns were designed essentially only for gravity loads as was practice in the 1970s. Using uncracked section properties the resulting fundamental period of the bare frame structure is approximately 1 s (0.98 s).

If a 13 cm thick infill wall is added to one bay on all floors the period reduces to 0.43 s. The stiffness of the infill panels has been estimated using the model developed by Crisafulli (CRIS 1997). The Young's Modulus of the masonry equals to 4 GPa and Poisson's ratio to 0.3. The density has been set to 1,600 kg/m^3. The importance of this change in period becomes evident when taking a look at Fig. 9 where the response spectrum of the North–South component is presented and both periods are marked.

The reduction in period increases the base shear by a factor of 4!

The majority of the base shear force is taken by the infill wall corresponding to its contribution to the overall stiffness. In this particular example the infill wall at ground level takes approximately 3,000 kN i.e. 4/5 of the total base shear force. The resulting average tangential stresses are higher than 4 N/mm^2 exceeding clearly the strength of conventional masonry.

In Fig. 10 three force time histories are presented, the total base shear and the parts that are taken by the infill wall and the frame structure, respectively.

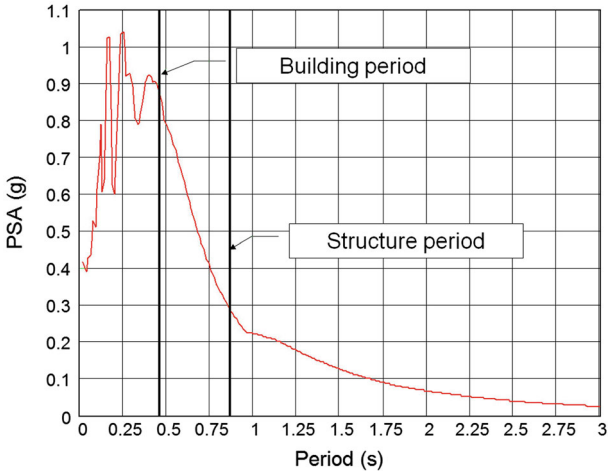

Fig. 9 Response spectrum of the North–South component of the Lorca earthquake

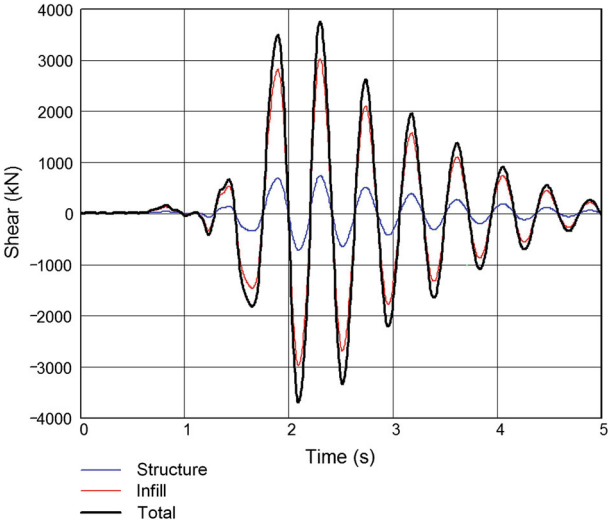

Fig. 10 Base shear force time histories

The force time histories displayed in Fig. 10 are the result of a linear elastic analysis so, in effect they are only valid till the failure of the infill walls. After the failure the structural behavior becomes much more complex requiring the use of more sophisticated models.

The intact infill panel reduces the fundamental period of the structure which results in considerable seismic forces that finally cause the failure of the masonry infill at a quite early stage of the earthquake.

This simple example may explain the high number of damages observed in infill and partition walls (see Fig. 11).

In order to study what happens after the failure of the masonry infill at ground level its stiffness is drastically reduced and the transient dynamic analysis is repeated i.e. the damaged structure is subjected to the seismic loads that result from the North–South component of the

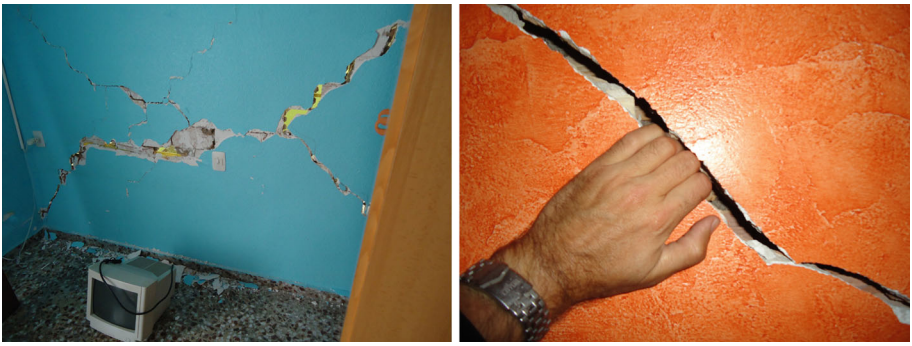

Fig. 11 Examples of damaged partiton walls during the Lorca earthquake

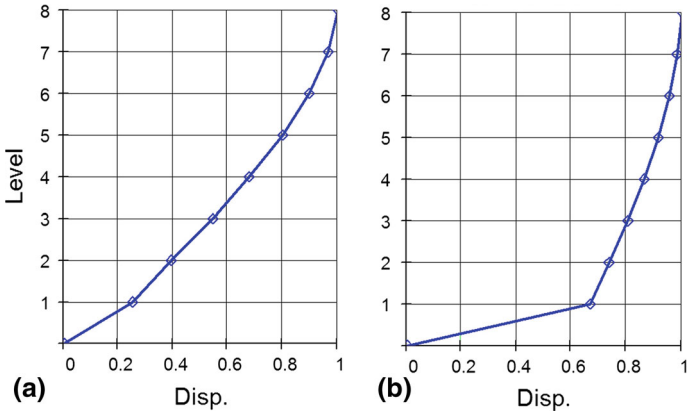

Fig. 12 *Mode shapes* of the building with intact (**a**) and with damaged (**b**) masonry infill wall at ground level

Lorca earthquake. The resulting fundamental period is 0.68 s and the maximum base shear force reaches 2,460 kN. The modification of the stiffness of the model drastically changes the mode shape as can be seen in Fig. 12.

In Fig. 12a the mode shape corresponding to the model with intact infill panel at ground level is shown and in Fig. 12b the one corresponding to the model with the damaged infill panel at ground level. In Fig. 13 an example is presented where two buildings pounded resulting in damaged façade elements. Pounding occurred at the floor level of the first floor as a consequence of the reduced lateral stiffness of the ground floor of one of the buildings. The reduction in stiffness was due to a cracked infill panel at ground level.

3.2 Column failure

The interaction between the infill panels and the surrounding frame structure during a seismic event is an active research topic and quite challenging to simulate. At the design stage of many of the existing buildings in Lorca, however, this interaction was taken into account only approximately if at all. As a consequence the columns i.e. the most important structural elements for gravity loads are subjected to loads that they were not designed for. In this

Fig. 13 Example of buildings that suffered damage due to pounding effects

context, it is worth to remember that according to (Moehle et al. 2008) column shear failure is the most frequently cited cause of concrete building failure and collapse in earthquakes!

Depending on the failure mode of the infill panel different types of loads at different locations act on the columns. In many cases the resistance of the infill panels is small enough so that the forces that have to be transferred to the frame structure can be supported without any problem. However, there is still the problem of the significant falling hazard related to a damaged infill panel. The situation is different if the infill panels are capable of supporting high loads. Due to the high in plane stiffness of the masonry infill the forces that have to be redistributed i.e. transferred from the infill to the frame structure are very important. In addition, the load redistribution occurs very rapidly and this fact contributes to the generation of brittle failures of columns. Today's design criteria (EN1998-1 2004) as well as standard text books on the seismic design of reinforced concrete and masonry buildings like (Paulay and Priestley 1992) insist that brittle failures of structural elements shall be avoided.

In very few cases the frame structure failed whereas the infill panels were intact after the earthquake.

In some cases both the frame structure and the infill panel showed similar resistance values so that the origin and sequence of failure could not exactly be identified.

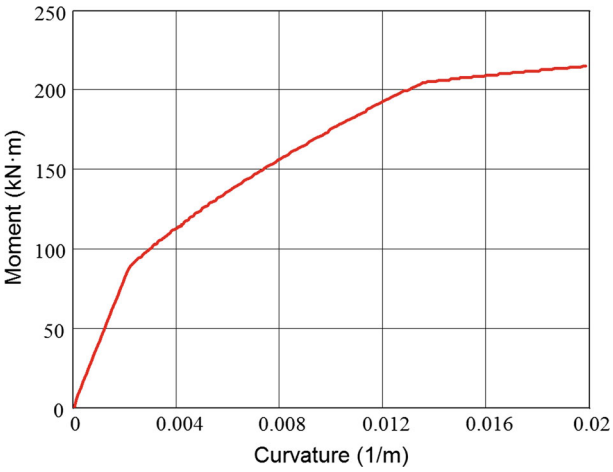

Fig. 14 Moment–curvature diagram of the compressed column

Fig. 15 Estimation of the shear demand in a column

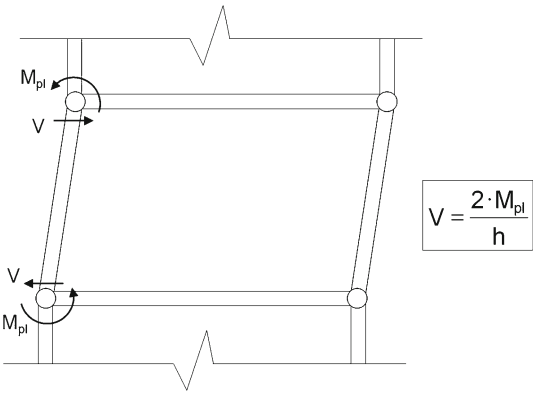

As example, suppose a concrete column of width 40 cm with quadratic section and a compressive strength of 25 MPa (5 % cylinder strength f_{ck}) that is reinforced with 3 bars of diameter 16 mm on each face subjected to an axial load that results in an average compressive stress of 5 MPa. In Fig. 14 the corresponding moment-curvature diagram is displayed.

The maximum value reaches 215 kNm. Based on equilibrium considerations of the capacity design method, see Fig. 15, and considering a floor height h of 4 m, the corresponding maximum shear force is 107.5 kN.

The shear capacity of this column without shear reinforcement is according to the Spanish Seismic Design Code (Norma de Construcción Sismoresistente 2002) 182.5 kN. Considering the same limit values for the maximum moment and the shear capacity of the column a floor height of 2.36 m would be necessary to increase the shear demand to an extent that the shear capacity is exceeded when reaching the maximum moment. However, this floor height is much lower than the limit value established by the urban building standards. This means that, in general, in the case of bare frames a column shear failure may be avoided if the capacity design approach is followed and properly detailed shear reinforcement is designed and provided. However, the situation is different in the case of infilled frames because magnitude and

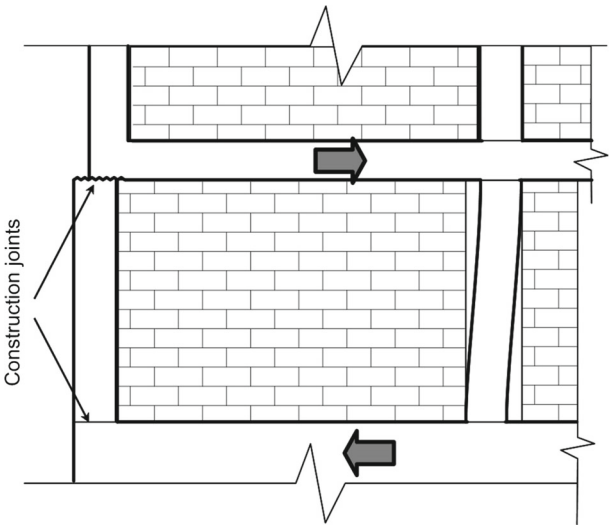

Fig. 16 Failure at the construction joint of beam–column connection

distribution of the contact forces between the infill wall and the surrounding frame are much more difficult to estimate.

In the following section the interaction between frame structure and infill panels will be further investigated.

4 Interaction of frame structure and infill panel

The numerical simulation of whole buildings in their elastic and post-elastic phases up to failure is even today quite challenging. Usually macro models are used when whole structures are analyzed whereas micro models are only employed when laboratory tests of structural elements are simulated. When using macro models it should be remembered that these models are generally unable to capture some of the failure modes described in the following.

4.1 Failure of the beam–column junction

Joints are usually critical points in structures and many efforts have been put into the study of its behavior. The importance of an adequate design is widely recognized however, quality control during construction is also very important.

Construction joints in columns are usually located at the undersides of the slabs and beams as shown in Fig. 16.

Failures of the contact surface were observed in several occasions (see Fig. 17).

This type of failure was observed particularly often in end bays of the exterior RC frames.

4.2 Sliding shear failure along mortar joints

This type of failure is particularly dangerous because of the damage that is caused to the compression zone of the infill panel, the load carrying strut in an equivalent strut model. This type of failure occurs when the shear bond strength of the mortar is lower than the shear

Fig. 17 Examples of failure at the construction joint of a beam–column connections

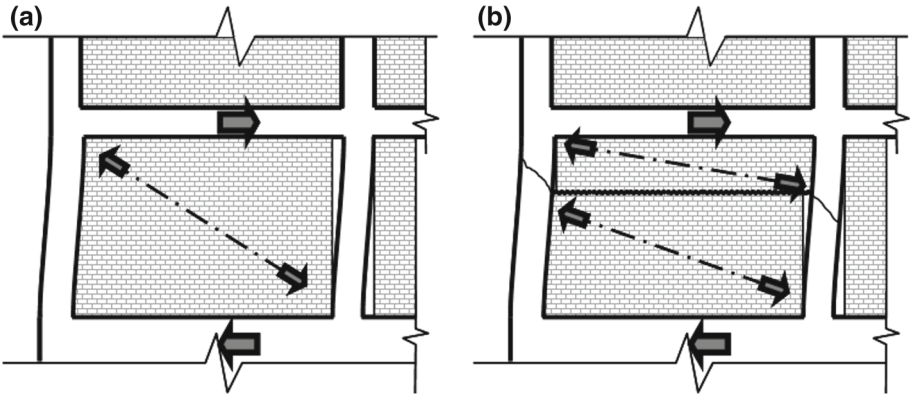

Fig. 18 Force transmission before (**a**) and after (**b**) sliding shear failure along a mortar joint

Fig. 19 Example of a shear–damaged column due to the failure of the adjacent infill panel

strength of the bricks. Sometimes this is the result of poor execution quality. If the failure results in the formation of two struts like indicated in Fig. 18b important forces act on the column sections almost at mid height of the floor.

The formation of two struts may be favored by the existence of conduits, openings or other discontinuities in the infill panel (see Fig. 19).

Fig. 20 Example of cracks crossing a column at mid-floor height. **a** Building, **b** detail

Table 2 Column dimensions and clear floor heights as a function of floor number (building 1)

Floor	1	2	3	4	5	6	7	8
Exterior column: width (cm)	45	45	40	40	35	35	35	30
Interior column: width (cm)	55	55	45	45	40	40	40	30
Clear floor height (cm)	395	295	295	295	295	295	295	295

4.3 Failure of the column and the infill panel

In general crack propagation in the infill panels indicates the position of the traction diagonal that connects two beam–column connections however, in some cases the cracks in the infill panels developed laterally displaced crossing the column at mid height like in Fig. 20b.

5 Push-over analysis of an eight-floor apartment building

In order to study the interaction between the frame structure and the masonry infill in more detail Finite Element models of two eight-floor apartment buildings have been set up. The first one is representative of current building practice and the second one is an example of structures built between 1960 and 1980. In Fig. 21 two views of the Finite Element Mesh corresponding to the first one are presented.

All columns have quadratic cross sections. The column dimensions vary as a function of the floor number. In addition the exterior columns have usually a smaller cross section than the interior ones. The dimensions are given in Table 2.

The beam depth is constant and amounts to 30 cm. Additional mass is added to the beams to account for the self weight and live loads that act on the floors. Columns, beams and the masonry infill walls are modeled using 8 node brick elements. The material properties used for masonry and concrete are given in Table 3.

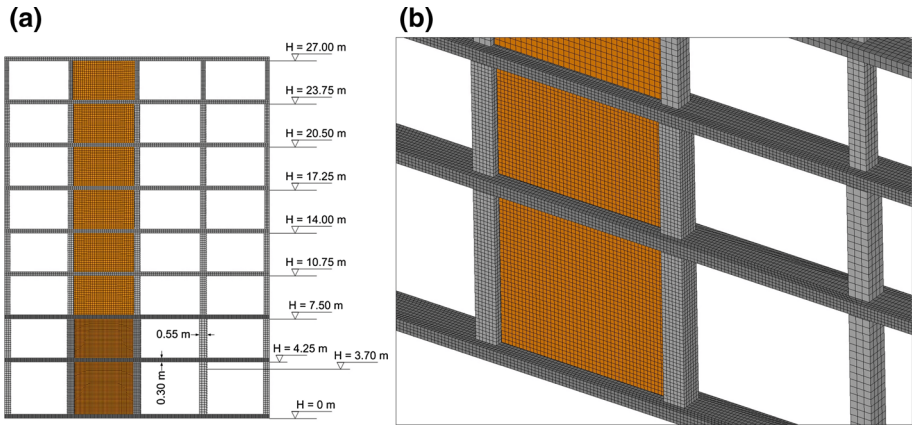

Fig. 21 Views of the Finite Element Mesh of building 1. **a** Elevation, **b** close-up

Table 3 Material properties used in the Finite Element model

Material	Concrete	Masonry
Young's modulus (GPa)	27	4
Poisson	0.25	0.3
Density (kg/m^3)	2,500	1,600

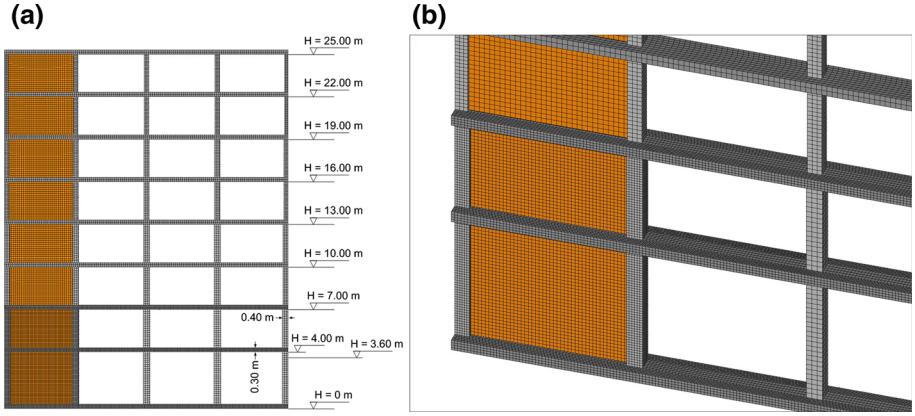

Fig. 22 Views of the Finite Element Mesh of building 2. **a** Elevation, **b** close-up

The infill wall thickness of 15 cm is the same on all floors. The shear strength at which crack initiation occurs in the infill walls has been fixed to 0.4 MPa. Contact elements are located between the frame structure and the infill panels to allow for gap opening. The stiffness of the contact elements perpendicular to the contact surface is almost infinite and a tangential friction coefficient of 0.15 has been used.

Regarding the second building the beam depth and span lengths are the same whereas the clear height of the ground floor is 4 m and that of the others 3 m. As can be seen in Fig. 22, the infill walls are located at the left end bay.

The dimensions are given in Table 4.

Table 4 Column dimensions and clear floor heights as a function of floor number (building 2)

Floor	1	2	3	4	5	6	7	8
Exterior column: width (cm)	40	40	35	35	30	30	25	25
Interior column: width (cm)	45	45	40	40	35	35	30	30
Clear floor height (cm)	370	270	270	270	270	270	270	270

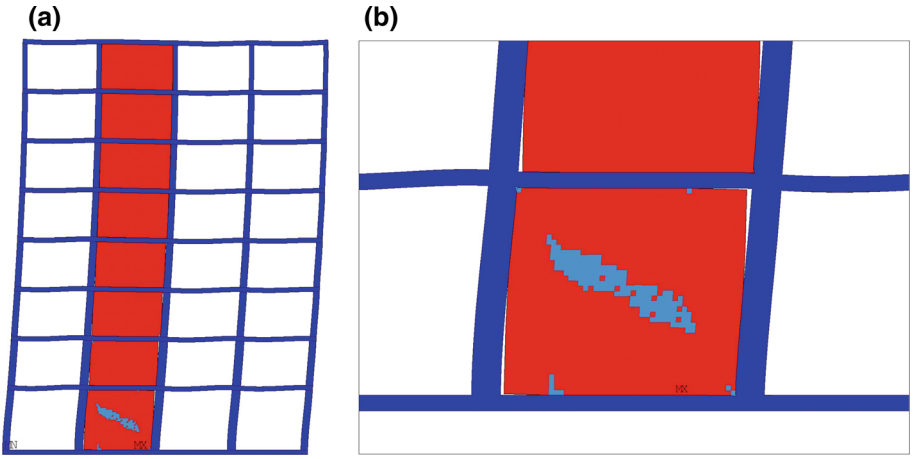

Fig. 23 Building 1: **a** Front view of the deformed structure; **b** Detail of the infill wall at ground floor level

The movement of all dof at the ground level was constrained by imposing zero displacements. At the beginning of the Push–Over analysis gravity loads are applied. The displacement pattern imposed during the Push–Over analysis follows a quarter sine wave starting from zero displacement at the ground and reaching the maximum value at the top of the building. The displacements are only imposed on the beams.

At each time step the shear forces at the top of the ground floor columns as well as the shear forces transmitted by the masonry infill wall at the same height are determined. In addition the shear forces one column width below the top of the ground floor columns are determined.

In Fig. 23 the configuration is shown when a diagonal crack forms in the infill panel. At this stage the relative displacement of the ground-storey is 5.3 mm which corresponds to a lateral drift of 0.12 %.

In Fig. 23b open gaps of up to 1.7 mm between the infill wall and the surrounding frame are clearly visible as well as the diagonal crack that develops in the infill panel. In Fig. 24 the contact pressures between masonry infill and columns are presented.

The maximum contact pressure is located very close to the construction joint of the column i.e. just below the beam soffit.

In Fig. 25 the Push–Over curve and the distribution of the shear forces are presented. Due to the presence of the infill panel column 2 transmits more than 60 % of the total base shear. A comparison of this value with the shear force transmitted by column 4, which amounts to 11 % of the total base shear, reveals the effect of the presence of an infill panel on column shear demands at the beam column junction. It is interesting to note that at this section only 10.5 % of the total base shear is transmitted by the infill wall. Things change if one considers

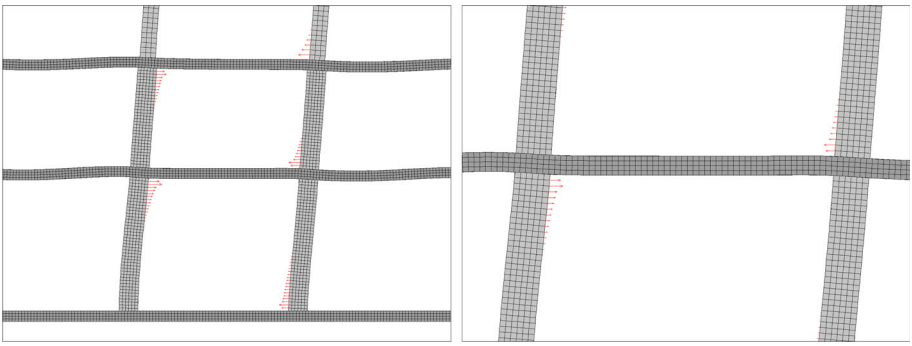

Fig. 24 Building 1: contact pressures between masonry infill and columns

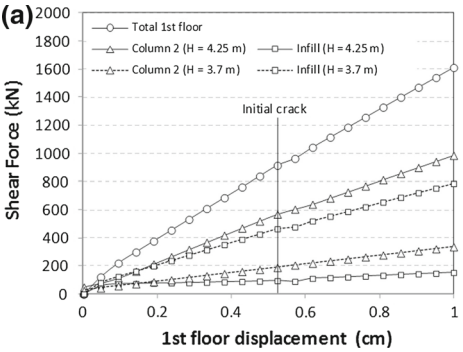

(b)

	H = 4.25 m		H = 3.7 m	
	Shear Force kN	Ratio %	Shear Force kN	Ratio %
Column 1	38.9	4.3%	38.9	4.3%
Column 2	569.2	62.2%	189.9	20.8%
Column 3	61.0	6.7%	61.0	6.7%
Column 4	98.9	10.8%	98.9	10.8%
Column 5	50.7	5.5%	50.7	5.5%
Infill	96.2	10.5%	475.5	52.0%
Total	915.0	100.0%	915.0	100.0%

Fig. 25 Building 1: **a** Push–Over curve, **b** shear force distribution at base

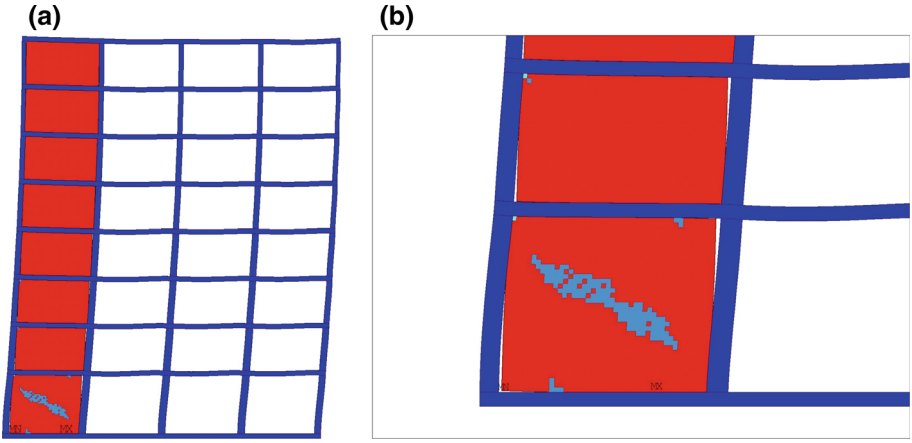

Fig. 26 Building 2: **a** Front view of the deformed structure; **b** Detail of the infill wall at ground floor level

the section located one column width below the top of the ground floor columns. In this case the column shear demand reduces to 20 % of the total base shear whereas the infill wall transmits 52 %.

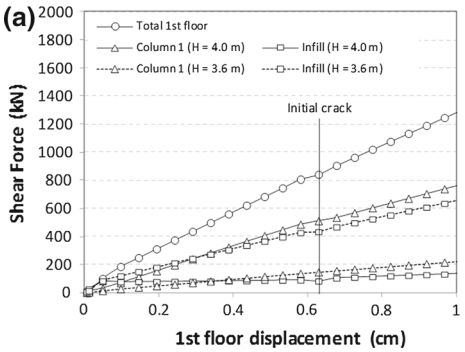

(b)

	H = 4.0 m		H = 3.6 m	
	Shear Force kN	Ratio %	Shear Force kN	Ratio %
Column 1	514.0	61.1%	149.0	17.7%
Column 2	41.9	5.0%	41.9	5.0%
Column 3	76.3	9.1%	76.3	9.1%
Column 4	76.3	9.1%	76.3	9.1%
Column 5	49.6	5.9%	49.6	5.9%
Infill	83.3	9.9%	448.2	53.3%
Total	841.4	100.0%	841.4	100.0%

Fig. 27 Building 2: **a** Push–Over curve, **b** shear force distribution at base

In Fig. 26 the configuration is shown when a diagonal crack forms in the infill panel. Due to the lower stiffness of the lateral resistance system the relative displacement of the ground-storey is higher and reaches 6.3 mm which corresponds to a lateral drift of 0.16 %. In this case open gaps of up to 2 mm form between the infill wall and the surrounding frame.

In Fig. 27 the Push–Over curve and the distribution of the shear forces corresponding to building 2 are presented.

The distribution of the shear force transmission is very similar to the one corresponding to building 1. At the section located just below the beam soffit the column shear demand amounts to more than 60 % of the total base shear whereas the shear force in a section 40 cm below is reduced to 17.7 %.

6 Shear failure of columns

In Sect. 3 the observed failure patterns of the buildings in Lorca have been described and in Sects. 2 and 5 the shear demands in the columns of a typical eight-floor building have been estimated. In what follows two failure modes will be further studied in more detail. The first one corresponds to the failure of the beam–column junction (section A–A′ in Fig. 28) and the second one to a conventional shear failure (shear failure plane A–A″) across an inclined shear-failure plane.

The capacity to prevent a sliding shear failure (section A–A′) at the beam column junction described in Sect. 3.2 is according to the Spanish design code for concrete structures (EHE 2008) 769 kN. On the other hand the shear capacity of the column without shear reinforcement (section A–A″) is 182.5 kN i.e. approximately 24 % of the former one. Neglecting a possibly existing transverse reinforcement in the columns is motivated by the fact that buildings from the 1960 to 1980s were usually not provided with amounts of transverse reinforcement that could significantly contribute to the overall shear capacity of the section. However, in Lorca as well as in L'Aquila (Verderame et al. 2011) sliding shear failures like that in section A–A′ occurred several times. Repeating the calculation of both capacity values for different types of concrete and column dimensions results in similar differences between both capacities. Several reasons may be given to explain the occurrence of sliding shear failures at the beam column junction. Insufficient quality control during the execution of the beam column junction may be responsible for much lower capacity values or a redistribution of gravitational forces from the columns to the infill walls as consequence of creep of the beams and shrinkage in

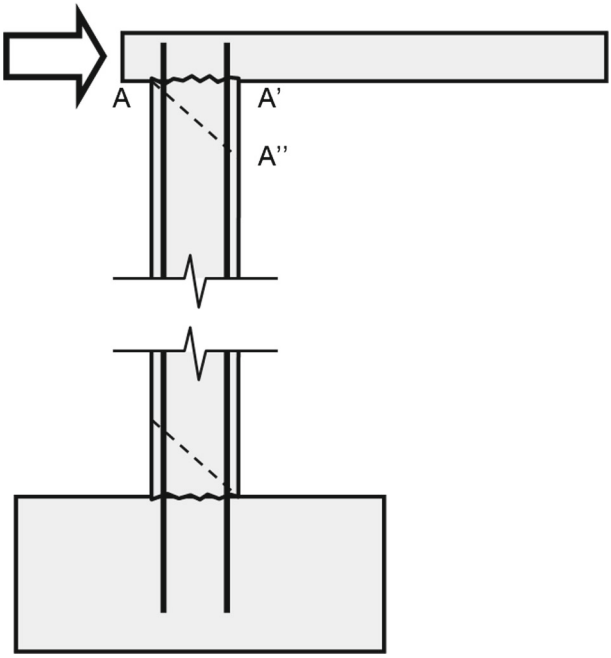

Fig. 28 Definition of the studied shear failure modes of columns

the columns. Note that this type of load transfer implies a reduction of the shear capacities of the columns as its axial loads decrease. However, the most likely reason for the occurrence of sliding shear failures at the beam column junction is thought to be a stress concentration at the corner due to the interaction of the infill wall and the surrounding frame. In Fig. 29 a sketch of the acting forces and the pressure distribution that acts just below the beam soffit is presented. In this case the shear forces at the two sections A–A′ and A–A″ are quite different.

7 Conclusions

The damages caused by the Lorca earthquake to structures that were built during the last 20 years indicate that lessons that should have been learned from previous seismic events have been, at least partially, ignored or misinterpreted. If RC frames are built with infill walls but their effect is not accounted for during design calculations and the structural analysis, the consequences may be catastrophic.

The differences in stiffness and ductility between the structural model (without infill) and the built structure can be very large. As masonry infill walls may significantly affect the way in which the building responds to the seismic event it should not be surprising that some buildings collapse although the magnitude of the earthquake is not very high. In this case the seismic loads that are used to analyze the seismic response of the structure may vary significantly from what the building will be subjected to. As a consequence of using erroneous design loads the members' ductility and resistance may result insufficient even for moderate earthquakes. This raises the question whether the seismic load case has been adequately studied. It has been demonstrated that column shear demand can vary very

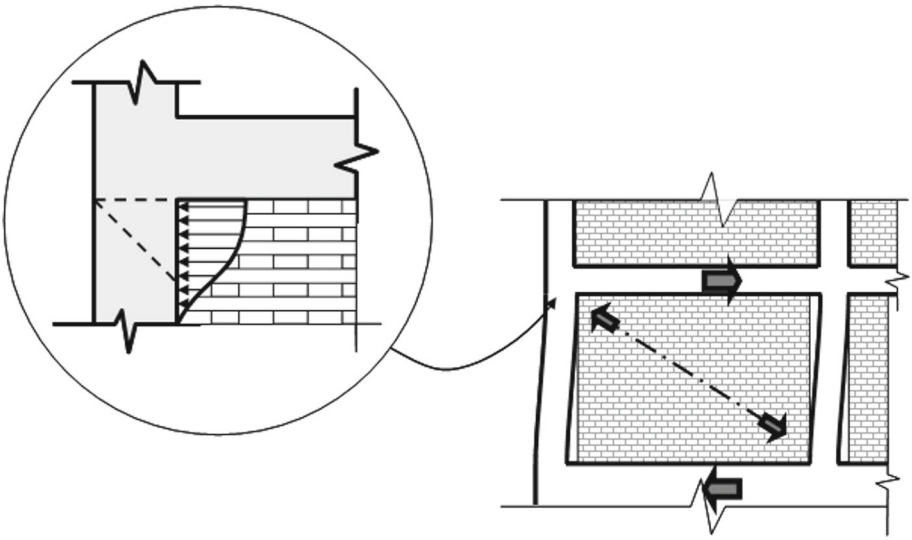

Fig. 29 Forces acting on the beam column junction according to the equivalent strut model

significantly close to the beam column junction as consequence of the interaction between the infill wall and the surrounding frame structure.

If the masonry infill panels are not included in the structural model that is used to study the seismic behavior of the building the non-structural infill walls should be designed and built with gaps to accommodate frame drifts; this solution is also known as isolated infill. When opting for this solution, the infill panels have to be provided with sufficient connections to avoid its falling out of their surrounding frames as a result of excessive lateral accelerations normal to their plane. Obviously these measures have an impact on the cost-effectiveness of the infill solution.

The falling hazard of damaged parapet walls is well known and addressed in several guidelines like (FEMA E-74 2011). The importance of non-structural elements in the context of a seismic analysis should be evaluated taking into account their damage potential. If this is considered high, the study of their seismic behavior should be mandatory.

References

Crisafulli FJ (1997) Seismic behaviour of reinforced concrete structures with masonry infills. PhD Thesis, Deparment of Civil Engineering, University of Canterbury

EHE (2008) Instrucción de Hormigón Estructural. Ministerio de Fomento. Publicación NIPO: 161–11-150-2, ISBN 978-84-498-0825-8 (www.fomento.es)

EN Code on Structural Concrete (EHE-08) (2008) Ministerio de Fomento (http://www.fomento.gob.es/MFOM/LANG_CASTELLANO/ORGANOS_COLEGIADOS/CPH/instrucciones/EHE08INGLES/)

EN1998-1 (2004) Eurocode 8: Design of structures for earthquake resistance. Part 1 General rules, seismic actions and rules for buildings. European Committee for Standardization

FEMA E-74 (2011) Reducing the risks of nonstructural earthquake damage: a practical guide, Fourth Edition (www.fema.gov)

Instituto Geográfico Nacional (2011) Informe del sismo de Lorca del 11 de mayo de 2011. (www.ign.es/ign/resources/sismologia/Lorca.pdf)

Moehle JP., Hooper JD., Lubke CD (2008) Seismic design of reinforced concrete special moment frames: a guide for practicing engineers. NEHRP Seismic Design Technical Brief No. 1

Norma de Construcción Sismoresistente (2002) Parte general y edificación. Ministerio de Fomento, España (www.fomento.es)

Paulay T, Priestley MJN (1992) Seismic design of reinforced concrete and masonry buildings. Wiley Interscience, New York. ISBN: 0-471-54915-0

Verderame GM, Luca F, Ricci G, Manfredi G (2011) Preliminary analysis of a soft-storey mechanism after the 2009 L'Aquila earthquake. Earthq Eng Struct Dyn